Syntheses and Crystal and Molecular Structures of the Hexakis(*N*,*N*-dimethylformamide) Complexes of Ruthenium(II) and Ruthenium(III)

Robert J. Judd,[†] Renhai Cao,[†] Margret Biner,[†] Thomas Armbruster,[‡] Hans-Beat Bürgi,[‡] André E. Merbach,[§] and Andreas Ludi*[,†]

Institut für Anorganische Chemie, Universität Bern, CH-3000 Bern 9, Switzerland, Laboratorium für Kristallographie, Universität Bern, CH-3012 Bern, Switzerland, Institut de chimie minérale et analytique, Université de Lausanne, Bâtiment de chimie, CH-1015 Lausanne, Switzerland

Received March 3, 1995[⊗]

Complexes $Ru(DMF)_6^{n+}$ ($n = 2, 3$; DMF = *N*,*N*-dimethylformamide) are prepared by a direct and simple synthesis from commercially available $RuCl_3 \cdot xH_2O$ and characterized by UV−vis, NMR, and cyclic voltammetry. Crystal and molecular structures are presented for $[Ru(DMF)_6](CF_3SO_3)_3$ (**I**) and $[Ru(DMF)_6](CF_3SO_3)_2$ (**II**). **I** is monoclinic, of space group $P2_1/c$, with $a = 18.28(1)$ Å, $b = 18.62(1)$ Å, $c = 13.29(1)$ Å, $\beta = 100.8(1)°$, $V = 4443(5)$ Å^3, $Z = 4$, $d_{calc} = 1.495$ g cm^{-3}, and $d_{obs} = 1.49$ (25 °C) g cm^{-3}. $R = 0.061$ ($R_w = 0.061$) for 4506 independent observed reflections with $I > 3\sigma(I)$. **II** is triclinic, of space group $P\bar{1}$, with, $a = 8.799(2)$ Å, $b = 9.557(2)$ Å, $c = 11.627(2)$ Å, $\alpha = 76.11(2)°$, $\beta = 84.73(2)°$, $\gamma = 85.12(2)°$, $V = 943.1(3)$Å^3, $Z = 1$, $d_{calc} = 1.475$ g cm^{-3}, and $d_{obs} = 1.477$ (25 °C) g cm^{-3}. $R = 0.061$ ($R_w = 0.058$) for 5189 independent observed reflections with $I > 3\ \sigma(I)$. Metal to ligand coordination is through the oxygen atom with average Ru−O distances of 2.02(1) Å (**I**) and 2.088(9) Å (**II**) in the octahedral units. The reduction potential for **I** measured by cyclic voltammetry is 0.28 V *vs* NHE.

Introduction

$[Ru(DMF)_6](CF_3SO_3)_3$ (**I**) and $[Ru(DMF)_6](CF_3SO_3)_2$ (**II**) were first synthesized using $[Ru(H_2O)_6](tosylate)_2$ as a starting material.[1,2] Both complexes are soluble in a variety of non-aqueous solvents, and **II** has been used as a starting reagent in the synthesis of macrocyclic amine complexes[2−6] and phosphine oxide complexes.[6,7] The use of **I** or **II** as starting material offers several advantages over $RuCl_3 \cdot H_2O$ or $Ru(H_2O)_6^{2+}$. **I** and **II** are well-characterized species in contrast to $RuCl_3$, where the oxidation state of the metal and hydration of the compound are ill-defined.[8,9] Moreover, due to the inertness of the Ru−Cl bond, products often retain Cl as a ligand, making homoleptic complexes hard to synthesize. In reactions involving water-insoluble or basic ligands such as phosphines or amines, $[Ru(H_2O)_6]^{2+}$ cannot be used because of deprotonation of the aqua ligand and subsequent decomposition of the starting material.[1,2] **I** and **II** do not show these difficulties. We present improved syntheses for **I** and **II** directly from $RuCl_3 \cdot xH_2O$ together with crystal and molecular structures for **I** and **II**.

Experimental Section

A. Syntheses. DMF (Merck, p.a.) and ether (Merck, rein) were used as received. DMF-*d7* (Chemie Uetikon AG, 99.5% D) was purified by literature methods.[10] $RuCl_3$ (42.1% Ru) was supplied by Johnson-Matthey. All gases were supplied by Carbagas. All elemental analyses were carried out by CIBA, Basel.

$[Ru(DMF)_6](CF_3SO_3)_3$ (I). $RuCl_3 \cdot xH_2O$ (500 mg) was dissolved in DMF (40 mL) with a catalytic amount of Pt black (Fluka, Puriss, 1−2 mg), and the mixture was saturated with hydrogen (3 h) to form a blue solution. $AgCF_3SO_3$ (Fluka, Ag >98%, 2.16 g) was added to the solution which was then refluxed with stirring (40 min, 153 °C) under Ar. The mixture was slowly cooled to 0 °C and then filtered (G4 glass frit) to remove AgCl from the yellow solution. The volume was reduced to 20 mL under reduced pressure (50 °C), and the solution was then added dropwise to rapidly stirred diethyl ether (500 mL). Filtration (G4 frit) afforded a yellow powder which was washed with diethyl ether (3 × 20 mL) and dried *in vacuo* (yield: 90%). Recrystallization from ethanol (50 °C) with slow cooling to −20 °C produced a microcrystalline sample of **I** (yield: 73%). Anal. Calcd (found) for $[Ru(C_3H_7NO)_6](CF_3SO_3)_3$: C, 25.44 (25.93); H, 4.32 (4.48); N, 8.48 (8.38); S, 9.70 (9.36); F, 17.24 (17.22). **I** was stored under ambient conditions in a desiccator. Yellow single crystals of $[Ru(DMF)_6](CF_3SO_3)_3 \cdot THF$ (**I**) suitable for X-ray diffraction were obtained by vapor diffusion of tetrahydrofuran (THF) into a DMF solution of the compound. Analytical data are consistent with one molecule of THF per formula unit.

$[Ru(DMF)_6](CF_3SO_3)_2$ (II) was prepared by dissolving **I** (300 mg) in DMF (20 mL) in the presence of Pt black (Fluka, Puriss, 3 mg) and saturating with hydrogen gas (2 h). The resulting red solution was filtered, and ether (30 mL) was added to precipitate red-orange crystals of **II**. The crystals were filtered off (G4 frit), washed with ether under Ar, and then dried *in vacuo* (yield: 90%). Anal. Calcd (found) for $[Ru(C_3H_7NO)_6](CF_3SO_3)_2$: C, 28.67 (28.42); H, 5.05 (4.99); N, 10.03 (9.96); S, 7.66 (7.61); F, 13.61 (13.76). **II** can be stored under Ar at −20 °C for more than a month without decomposition. Red single crystals of $[Ru(DMF)_6](CF_3SO_3)_2$ (**II**) were obtained by slow diffusion of ether into a concentrated DMF solution of the compound under argon.

B. Crystal Structure Analyses of $[Ru(DMF)_6](CF_3SO_3)_3 \cdot THF$ (I) and $[Ru(DMF)_6](CF_3SO_3)_2$ (II). Collection and Reduction of the Diffraction Data. A crystal of **I** was sealed in a Lindemann capillary together with a small amount of the THF solvent. A crystal of **II** was mounted on a quartz fiber along the longest dimension (*a* direction), and the fiber was placed in a Lindemann glass capillary which was sealed under dry argon. Both crystals were of approximately prismatic shape. Data collection was carried out on an Enraf-Nonius four-circle

[†] Institut für Anorganische Chemie, Universität Bern.
[‡] Laboratorium für Kristallographie, Universität Bern.
[§] Université de Lausanne.
[⊗] Abstract published in *Advance ACS Abstracts,* September 1, 1995.
(1) Bernhard, P.; Lehmann, H.; Ludi, A. *Comments Inorg. Chem.* **1983**, *2*, 145.
(2) Bernhard, P.; Sargeson, A. M. *J. Chem. Soc., Chem. Commun.* **1985**, *21*, 1516.
(3) Bernhard, P.; Sargeson, A. M. *Inorg. Chem.* **1988**, *27*, 2582.
(4) Bernhard, P.; Sargeson, A. M. *J. Am Chem. Soc.* **1989**, *111*, 597.
(5) Bernhard, P.; Bull, D. J.; Robinson, W. T.; Sargeson, A. M. *Aust. J. Chem.* **1992**, *45*, 1241.
(6) Keene, F. R.; Snow, M. R.; Stephenson, P. J.; Tiekink, E. R. T. *Inorg. Chem.* **1988**, *27*, 2040.
(7) Keene, F. R.; Stephenson, P. J.; Tiekink, E. R. T. *Inorg. Chim. Acta* **1991**, *187*, 217.
(8) Seddon, E. A.; Seddon, K. R. *The Chemistry of Ruthenium*; Elsevier: Amsterdam, 1984.
(9) Hui, B. C.; James, B. R. *Can. J. Chem.* **1974**, *52*, 348.

0020-1669/95/1334-5080$09.00/0 © 1995 American Chemical Society

Table 1. Crystallographic Data for $[Ru(DMF)_6](CF_3SO_3)_3$·THF (**I**) and $[Ru(DMF)_6](CF_3SO_3)_2$ (**II**)

	I	II
formula	$C_{25}H_{50}N_6O_{16}F_9S_3Ru$	$C_{20}H_{42}N_6O_{12}F_6S_2Ru$
fw	1058.94	837.77
cryst syst	monoclinic	triclinic
space group	$P2_1/c$ (No. 14)	$P\bar{1}$ (No. 2)
λ (Å)	0.710 69	0.710 69
a (Å)	18.28(1)	8.799(2)
b (Å)	18.62(1)	9.557(2)
c (Å)	13.29(1)	11.627(2)
α (deg)	90	76.11(2)
β (deg)	100.8(1)	84.73(2)
γ (deg)	90	85.12(2)
V (Å^3)	4443(5)	943.1(3)
Z	4	1
d_{obs}(flotation) (g cm^{-3})	1.49 (23 °C)	1.48
d_{calc} (g cm^{-3})	1.495	1.475
temp (K)	100	room temp
μ(Mo Kα) (cm^{-1})	5.40	5.37
F(000) (electrons)	2172	430
cryst dimens (mm)	0.46 × 0.41 × 0.34	0.57 × 0.39 × 0.28
scan mode	ω	ω
scan width (deg)	2 + 0.35(tan θ)	1.0 + 0.35(tan θ)
2θ range (deg)	0−50	0−60
h, k, l range	±21, 0−22, 0−15	±12, −13 to +13, 0−16
transm factors	max, 0.99; min, 0.96	max, 0.998; min, 0.964
no. of unique reflcns	5902	5457
no. of obsd reflcns with $I_o > 3\sigma(I_o)$	4506	5189
weighting scheme	unit weights	$W = 1/(\sigma^2(F) + 0.0030F^2)$
R^a	0.061	0.061
$R_w{}^b$	0.061	0.058
residual density (e Å^{-3})	+1.06 and −1.46	+0.94 and −0.90

$^a R = \Sigma(|F_o| - |F_c|)/\Sigma|F_o|$ $^b R_w = [\Sigma w(F_o^2 - F_c^2)/\Sigma wF_o^2]^{1/2}$.

CAD4 diffractometer at 100 K for **I** and at room temperature for **II** using Mo Kα radiation (0.710 69 Å, graphite monochromator). The standard liquid-nitrogen attachment was used for data collection of **I** at 100 K. The intensities of three standard reflections recorded every 60 min for **I** and 120 min for **II** during data collection did not show any systematic intensity fluctuations. In addition, three orientation standard reflections were recentered after 60 reflections to minimize the effects of crystal movement for **II** and **I**. Crystal **I** was fixed on the inside wall of the capillary with solvent which solidified at low temperature. During data collection, the orientation matrix was lost repeatedly, which indicated movement of the crystal. After reorientation, the data collection was continued. The intensity data for **I** and **II** were corrected for Lorentz−polarization effects, but only for **II** were they corrected for absorption effects. The SDP program by Frenz[11] was used for data reduction. No correction for extinction was applied.

Solution and Refinement of the Structures. Details of the crystal data and the intensity collection and refinement procedures for **I** and **II** are given in Table 1. Both crystal structures were solved by Patterson and Fourier methods and refined by full-matrix least-squares using the program SHELX 76.[10,11] The atomic scattering factors for ruthenium were obtained from ref 12[12] and for other atoms from SHELX 76.[13] ORTEP drawings were generated with XTAL2.4.[14]

For **I**, the Ru^{3+} atom occupies two independent sets of special positions in $P2_1/c$. Hydrogen positions of DMF were located in difference Fourier maps. The non-hydrogen atoms were refined anisotropically, and the hydrogen atoms were given a single isotropic temperature factor which refined to 0.04(1) Å^2. The refinement showed that the tetrahydrofuran molecule is disordered as is not uncommon for cocrystallized THF.[15] It was not possible to distinguish the oxygen atom in the THF molecule from the carbon atoms, and a carbon scattering factor was therefore assigned to all the five ring atoms. The hydrogen atoms of THF could not be located in the final difference maps and were not included in the least-squares refinement. In the final difference map there were two high peaks (+0.88 and +0.75 e/Å^3) around THF. One of the three $CF_3SO_3^-$ anions is also disordered. Around this $CF_3SO_3^-$ anion, several peaks of electron density (0.89, 0.86, 0.61, and 0.61 e/Å^3) were found in the final difference map. A number of unsuccessful attempts were made to improve the modeling of the anion as described below for **II**. Additional difference Fourier peaks were found (0.96, 0.90, 0.89, 1.06, 0.81, 0.80, and 0.68 e/Å^3) around the two independent Ru atoms. The noisy difference Fourier map is probably due to the experimental difficulties (see above) which also prevented a meaningful absorption correction to be made. Nevertheless, the molecular geometry (Table 4) is not expected to be significantly affected by these difficulties. The esd's obtained from the least-squares refinement seemed optimistic, and in Table 4 they have therefore been increased (somewhat arbitrarily) by a factor of 2.[16]

For **II**, all the non-hydrogen atoms of the cation and the anion were located in successive difference Fourier maps. Large displacement parameters and observed residual electron density in the vicinity of the anion presented evidence for structural disorder. The disorder was modeled by an overlay of two rigid molecules with variable population. The temperature factors were refined anisotropically for the $Ru(DMF)_6^{2+}$ cation and isotropically for the $CF_3SO_3^-$ anion until convergence was achieved. The methyl groups are disordered due to internal rotation about the N−C bond; they were modeled with six half-hydrogen atoms forming a hexagon. The refined atomic coordinates for the two structures are listed in Tables 2 and 3.

Results

Syntheses and Characterization. The direct synthesis of **I** and **II** from $RuCl_3{\cdot}xH_2O$ is a significant improvement over the previous route via $Ru(H_2O)_6^{2+}$. The addition of $AgCF_3SO_3$ to the Ru-blue solution scavenges the Cl^- and supplies the counterion. Ag^+ may oxidize the Ru mixture to Ru^{3+}. Both **I** and **II** are soluble in a range of nonaqueous solvents, including acetone, nitromethane, methanol, ethanol, acetone, dichloromethane, and dimethylformamide. Infrared spectroscopy shows[17] a decrease in the carbonyl frequency from 1673 cm^{-1} in free DMF to 1642 cm^{-1} in **I** and to 1635 cm^{-1} in **II**. Cyclic voltammetry (in 0.1 M tetrabutylammonium tetrafluoroborate)/DMF) of **I** shows a quasi-reversible redox couple at 0.12 V *vs* Ag/AgCl/KCl(satd), ΔE = 90 mV (Fc/Fc^+ = +0.54 V *vs* Ag/AgCl/KCl(satd), ΔE = 100 mV) equivalent to a reduction potential of 0.28 V *vs* NHE,[18] obtained for the Ru(III)/Ru(II) couple. The UV−vis spectrum of **I** (0.1 M, DMF) shows transitions with intensities characteristic of LMCT bands: 342 (5770), 272 (6970), and 254 (1730) nm (ϵ, M^{-1} cm^{-1}). The UV−vis spectrum of **II** (0.1 M, DMF) shows one transition at 494 nm with an intensity of 186 M^{-1} cm^{-1} characteristic of a d−d band which is assigned to the $^1A_{1g} \rightarrow {}^1T_{1g}$ transition of a d^6 low-spin complex.[19] The expected $^1A_{1g} \rightarrow {}^1T_{2g}$ transition is obscured by CT bands.

(10) Cossy, C.; Helm, L.; Merbach, A. E. *Helv. Chim. Acta* **1987**, *70*, 1516.
(11) Frenz, B. A. *Structure Determination Package*; Enraf-Nonius: Delft, The Netherlands, 1983.
(12) Cromer, D. T.; Waber, J. T. *International Tables for X-Ray Crystallography*; Kynoch Press: Birmingham, England, 1974.
(13) Sheldrick, G. *SHELX76, Program for Crystal Structure Determination*; University of Cambridge: Cambridge, England, 1976.
(14) Davenport, G.; Hall, S. R. ORTEP, Universities of Western Australia and Maryland, 1988; Version of G. Davenport and S. R. Hall in XTAL2.4.
(15) Rietz, R. R.; Edelstein, N. M.; Ruben, H. W.; Templeton, D. H.; Zalkin, A. *Inorg. Chem.* **1978**, *17*, 658.
(16) Taylor, R.; Kennard, D. *Acta Crystallogr.* **1986**, *B42*, 112.
(17) IR of **I** (KBr pellets): 1642 (s), 1350 (s), 1222 (m), 717 (s) cm^{-1}. IR of **II** (KBr pellets): 1635 (s), 1368 (s), 1221 (m), 1115 (m), 697 (m) cm^{-1}. These can be compared with IR of DMF(l): 1673 (s), 1387 (s), 1255 (m), 1090 (s), 655 (s) cm^{-1}.
(18) Both working and auxiliary electrodes were platinum, and Bu_4NPF_6 or Bu_4NClO_4 was used as supporting electrolyte (0. 1 M); [Ru] ≈ 2 mM; v = 30 mV s^{-1}.
(19) Bramley, R.; Brorson, M.; Sargeson, A. M.; Schäffer, C. E. *J. Am. Chem. Soc.* **1985**, *107*, 2780.

Table 2. Final Atomic Positional Parameters and B_{eq} Values for Non-Hydrogen Atoms, with Standard Deviations in Parentheses, for $[Ru(DMF)_6](CF_3SO_3)_2$ at 293 K[a]

atom	a/x	y/b	z/c	B_{eq},[b] Å^2
Ru	0	0	0	3.068(5)
O1	0.0734(3)	−0.2087(2)	−0.0186(2)	4.15(4)
C1	0.0973(4)	−0.2410(4)	−0.1144(3)	4.86(6)
N1	0.1593(4)	−0.3674(4)	−0.1283(4)	5.77(4)
C11	0.2086(6)	−0.4772(5)	−0.0315(5)	6.7(1)
C12	0.1794(9)	−0.407(1)	−0.2397(6)	11.0(2)
O2	0.0898(3)	−0.0495(2)	0.1662(2)	3.97(3)
C2	0.0817(4)	−0.1699(4)	0.2344(3)	4.34(5)
N2	0.1132(4)	−0.1982(4)	0.3457(3)	4.94(5)
C21	0.111(1)	−0.3423(6)	0.4209(5)	9.1(2)
C22	0.1600(7)	−0.0897(6)	0.3971(4)	6.9(1)
O(3)	−0.2029(3)	−0.0772(3)	0.0891(2)	4.26(4)
C3	−0.3004(3)	−0.1289(3)	0.0436(3)	3.74(4)
N3	−0.4293(3)	−0.1754(3)	0.0988(3)	4.60(5)
C31	−0.4669(6)	−0.169(1)	0.2193(5)	9.7(2)
C32	−0.5388(4)	−0.2347(4)	0.0419(4)	5.73(8)
SA	0.3010(4)	−0.6787(4)	0.2932(3)	6.95(4)*
SB	0.3318(5)	−0.6715(5)	0.2734(4)	6.95(4)*
O4A	0.369(1)	−0.5465(9)	0.256(1)	10.9(1)*
O5A	0.371(1)	−0.737(1)	0.234(1)	10.9(1)*
O6A	0.1515(8)	−0.686(1)	0.319(1)	10.9(1)*
O4B	0.441(1)	−0.585(1)	0.201(1)	10.9(1)*
O5B	0.271(1)	−0.770(1)	0.217(1)	10.9(1)*
O6B	0.198(1)	−0.574(1)	0.292(1)	10.9(1)*
C4A	0.374(1)	−0.737(1)	0.442(1)	11.9(3)*
C4B	0.390(1)	−0.751(1)	0.425(1)	11.9(3)*
F1A	0.348(1)	−0.876(1)	0.492(1)	12.9(1)*
F2A	0.301(1)	−0.654(1)	0.510(1)	12.9(1)*
F3A	0.522(1)	−0.730(1)	0.443(1)	12.9(1)*
F1B	0.277(1)	−0.822(1)	0.494(1)	12.9(1)*
F2B	0.434(2)	−0.650(1)	0.470(1)	12.9(1)*
F3B	0.505(1)	−0.838(1)	0.403(1)	12.9(1)*

[a] A, B indicate the two triflate anions. [b] Starred values denote that the atoms were refined isotropically. Anisotropically refined atoms are given in the form of the isotropic equivalent thermal parameter defined as $B_{eq} = {}^8/_3\pi^2[\sum_i\sum_j U_{ij}a_i^*a^*a_j^*a_ia_j]$.

NMR Spectra. The NMR chemical shifts of $[Ru(DMF)_6](CF_3SO_3)_2$ and $[Ru(DMF)_6](CF_3SO_3)_3$ obtained in DMF-d_7 are given in the footnotes.[20] The proton signals of the two methyl groups in DMF are separated by 0.17 ppm which on coordination of the ligand changes to 0.12 ppm for Ru^{2+} and 2.6 ppm for Ru^{3+}. There are considerable downfield shifts in the methyl group proton peaks of **I** and **II** in comparison to DMF. The high-field methyl resonance in bound and free DMF has been assigned to the methyl group *cis* with respect to the carbonyl oxygen atom.[21,22] The formyl signal for **I** was not found.

Molecular and Crystal Structures of $[Ru(DMF)_6](CF_3SO_3)_3$·THF and $[Ru(DMF)_6](CF_3SO_3)_2$. The structure of $Ru(DMF)_6^{2+}$ exhibits the expected octahedral coordination geometry with Ru−O bonding (O−Ru−O angles 89.0 (1), 90.1 (1), 86.6 (1)°). The Ru−O−C−N fragment shows a *trans* configuration (Ru−O=C angle 122.0−124.2°). All of the dimethylformamide molecules are planar within experimental error. The structure of $[Ru(DMF)_6](CF_3SO_3)_3$·THF contains two independent $Ru(DMF)_6^{3+}$ ions, both of which exhibit crystallographic ($\bar{1}$) symmetry. Figure 1 shows a PEANUT[23] diagram of one of the two independent $Ru(DMF)_6^{3+}$ octahedra. Selected bond lengths and angles for both structures are given in Table 4. The independent $Ru(DMF)_6^{3+}$ ions possess almost regular octahedral geometry (O−Ru1−O angles 90.3(4), 89.7(4), 88.3(4)°; O−Ru2−O angles 90.7(4), 88.9(4), 87.6(4)°). DMF is coordinated to ruthenium through oxygen with Ru−O−C−N in a *trans* conformation (Ru(1)−O=C angles 120−122°; Ru(2)−O=C angles 121−124°). For $[Ru(DMF)_6](CF_3SO_3)_3$·THF, the average ruthenium-oxygen distance, averaged over the two

Table 3. Final Atomic Positional Parameters and B_{eq} Values for Non-Hydrogen Atoms, with Standard Deviations in Parentheses, for $[Ru(DMF)_6](DMF)_6](CF_3SO_3)_3$·THF at 100 K

atom	a/z	y/b	z/c	B_{eq},[a] Å^2
Ru1	0	0	0	1.83(2)
Ru2	0.5	0	0.5	1.53(2)
O1	0.0787(3)	0.0718(3)	0.0609(4)	1.9(2)
C1	0.1389(5)	0.0769(4)	0.0271(6)	2.0(2)
N1	0.1874(4)	0.1269(3)	0.0545(5)	2.1(2)
C11	0.2541(6)	0.1330(5)	0.0112(9)	3.3(2)
C12	0.1716(7)	0.1831(6)	0.1249(8)	3.7(2)
O2	−0.0723(3)	0.0828(3)	−0.0335(4)	2.2(1)
C2	−0.0781(5)	0.1293(4)	0.0341(6)	2.4(2)
N2	−0.1132(4)	0.1892(4)	0.0116(5)	3.0(1)
C21	−0.1229(8)	0.2403(7)	0.0926(9)	5.1(3)
C22	−0.1483(7)	0.2077(6)	−0.0918(8)	3.9(2)
O3	0.0311(3)	0.0112(3)	−0.1379(4)	2.0(1)
C3	−0.0149(5)	0.0244(4)	−0.2182(6)	2.2(2)
N3	0.0052(4)	0.0362(4)	−0.3065(5)	2.3(1)
C31	0.0822(6)	0.0295(7)	−0.3172(7)	3.5(3)
C32	−0.0505(6)	0.0479(6)	−0.3998(7)	3.3(2)
O4	0.4964(3)	−0.0191(2)	0.3502(4)	1.9(1)
C4	0.4792(5)	0.0299(4)	0.2840(6)	2.0(1)
N4	0.4772(4)	0.0194(3)	0.1867(4)	1.9(1)
C41	0.4586(6)	0.0770(4)	0.1125(6)	2.6(2)
C42	0.4955(7)	−0.0488(5)	0.1445(7)	3.0(2)
O5	0.5593(3)	0.0895(3)	0.4836(4)	1.7(1)
C5	0.5377(5)	0.1509(4)	0.5104(5)	1.7(1)
N5	0.5666(4)	0.2096(3)	0.4833(5)	1.9(1)
C51	0.6210(6)	0.2107(5)	0.4170(8)	3.3(2)
C52	0.5396(6)	0.2789(4)	0.5131(8)	2.7(2)
O6	0.4061(3)	0.0588(3)	0.4670(4)	1.9(1)
C6	0.3499(5)	0.0483(4)	0.5066(6)	2.1(2)
N6	0.2897(4)	0.0859(4)	0.4884(5)	2.3(1)
C61	0.2842(6)	0.1488(5)	0.4200(8)	3.4(2)
C62	0.2255(6)	0.0713(6)	0.5360(9)	3.7(3)
S1	0.4115(2)	0.2616(1)	0.2237(2)	3.06(5)
O7	0.4814(4)	0.2974(3)	0.2374(4)	3.2(1)
O8	0.3746(4)	0.2560(4)	0.1198(5)	5.5(2)
O9	0.4113(5)	0.1973(3)	0.2840(6)	6.3(2)
C7	0.3516(5)	0.3215(4)	0.2793(6)	2.8(2)
F1	0.3471(3)	0.3856(3)	0.2343(4)	4.1(1)
F2	0.2832(3)	0.2960(3)	0.2736(4)	4.5(1)
F3	09.3778(3)	0.3334(3)	0.3796(3)	3.0(1)
S2	−0.2838(2)	0.0801(1)	0.0844(2)	3.46(5)
O10	−0.2825(4)	0.1479(4)	0.0371(6)	5.4(2)
O11	−0.3511(4)	0.0414(5)	0.0550(6)	7.1(2)
O12	−0.2154(4)	0.0427(5)	0.0950(7)	6.9(2)
C8	−0.2895(8)	0.090(1)	0.204(1)	12.8(8)
F4	−0.2313(7)	0.1398(6)	0.2566(7)	12.1(3)
F5	−0.2916(5)	0.0468(5)	0.2721(5)	9.0(2)
F6	−0.3517(7)	0.1325(7)	0.2179(6)	14.0(4)
S3	0.0389(1)	0.3380(1)	−0.1345(2)	2.98(5)
O13	0.0898(4)	0.3816(3)	−0.1808(5)	3.8(1)
O14	−0.0365(4)	0.3444(4)	−0.1755(7)	6.0(2)
O15	0.0569(4)	0.3382(4)	−0.0243(5)	5.1(2)
C9	0.0628(7)	0.2461(5)	−0.1638(8)	3.9(2)
F7	0.0459(4)	0.2347(3)	−0.2670(4)	5.6(1)
F8	0.0259(4)	0.1984(3)	−0.1209(5)	5.5(2)
F9	0.1340(3)	0.2331(3)	−0.1382(5)	4.6(1)
C10	0.7886(6)	0.0771(7)	0.6982(8)	4.5(3)
C11	0.7289(7)	0.1192(7)	0.6749(9)	5.4(3)
C12	0.6794(9)	0.1022(7)	0.750(1)	5.8(3)
C13	0.7755(8)	0.0213(8)	0.769(1)	7.2(4)
C14	0.7007(8)	0.0236(8)	0.775(1)	6.9(4)

[a] The thermal parameter given is the isotropic equivalent thermal parameter defined as $B_{eq} = {}^8/_3\pi^2[\sum_i\sum_j U_{ij}a_i^*a_j^*a_ia_j]$.

(20) DMF ^{1}H NMR (400 MHz, DMF-d_7): CH_3CH_3NCHO, s, 2.96 ppm; CH_3CH_3NCHO, s, 2.79 ppm; CH_3CH_3NCHO, s, 8.03 ppm. $[Ru(DMF)_6](CF_3SO_3)_2$ ^{1}H NMR (400 MHz, DMF-d_7): CH_3CH_3NCHO, s, 3.22 ppm; CH_3CH_3NCHO, s, 3.10 ppm; CH_3CH_3NCHO, s, 8.08 ppm. $[Ru(DMF)_6](CF_3SO_3)_3$ ^{1}H NMR (400 MHz, DMF-d_7): CH_3CH_3NCHO, s, 22.70 ppm; CH_3CH_3NCHO, s, 20.10 ppm; CH_3CH_3NCHO, not found.

(21) Matwiyoff, N. A. *Inorg. Chem.* **1966**, *5*, 788.

(22) Wayland, B. B.; Drago, R. S.; Henneike, H. F. *J. Am. Chem. Soc.* **1966**, *88*, 2455.

(23) Hummel, W.; Hauser, J.; Bürgi, H. B. *J. Mol. Graphics* **1990**, *8*, 214.

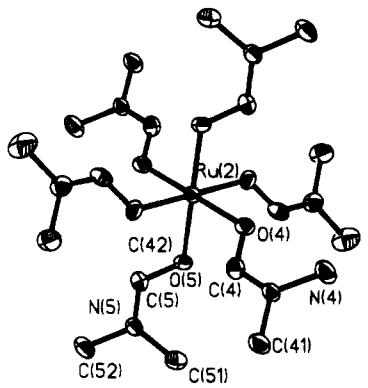

Figure 1. ORTEP diagram with labeling scheme for one of the two independent ions of $Ru(DMF)_6^{3+}$ (50 % probability thermal ellipsoids).

Table 4. Selected Bond Lengths (Å) and Angles (deg) for $Ru(DMF)_6^{3+}$ (**I**) and $Ru(DMF)_6^{2+}$ (**II**)

	I		II
	Ru1	Ru2	
Ru–O1	2.02(1)	2.01(1)	2.098(2)
Ru–O2	2.03(1)	2.02(1)	2.088(2)
Ru–O3	2.03(1)	2.01(1)	2.079(2)
O1–C1	1.27(3)	1.27(2)	1.221(4)
O2–C2	1.27(2)	1.28(2)	1.234(4)
O3–C3	1.25(1)	1.26(3)	1.241(4)
C1–N1	1.29(3)	1.30(2)	1.322(5)
C2–N2	1.29(3)	1.29(2)	1.308(4)
C3–N3	1.31(3)	1.29(3)	1.308(4)
N1–C11	1.45(3)	1.45(2)	1.414(6)
N1–C12	1.47(3)	1.45(3)	1.424(6)
N2–C21	1.47(3)	1.45(3)	1.443(5)
N2–C22	1.45(3)	1.46(3)	1.421(6)
N3–C31	1.45(3)	1.48(3)	1.425(6)
N3–C32	1.47(3)	1.46(3)	1.441(5)
O1–Ru–O2	88.3(4)	87.6(4)	89.0(1)
O1–Ru–O3	89.7(4)	90.7(4)	90.1(1)
O2–Ru–O3	90.3(4)	88.9(4)	86.6(1)
Ru–O1–C2	121(1)	121(1)	123.7(2)
Ru–O2–C2	120(1)	121(1)	122.0(2)
Ru–O3–C3	122(2)	124(1)	124.4(3)
O1–C1–N1	123(2)	123(2)	124.2(3)
O2–C2–N2	122(2)	121(2)	123.7(3)
O3–C3–N3	123(2)	125(2)	124.4(3)
C1–N1–C11	122(2)	122(2)	122.1(4)
C1–N1–C12	119(2)	123(2)	123.8(5)
C2–N2–C21	121(2)	123(2)	122.1(4)
C2–N2–C22	123(2)	120(2)	121.5(3)
C3–N3–C31	121(2)	120(2)	120.5(3)
C3–N3–C32	121(2)	123(2)	120.3(3)
C11–N1–C12	119(2)	115(2)	114.1(5)
C21–N2–C22	117(2)	117(2)	120.5(3)
C31–N3–C32	118(2)	117(2)	117.2(4)

independent octahedra, is 2.02(1) Å. The average Ru(II)–oxygen distance is 2.088(9) Å. The difference in metal–ligand bond distances between the two oxidation states is thus 0.07(1) Å.

Discussion

The synthesis of $[Ru(DMF)_6](CF_3SO_3)_3$ reported here is a more facile and efficient method than the previously published route via $Ru(H_2O)_6^{2+}$. The product is a useful alternative to $RuCl_3$ as a source of Ru in nonaqueous synthesis because of its solubility in a wide range of solvents and its ability to be stored for long periods at ambient temperature. Salts of $Ru(DMF)_6^{2+}$ can be synthesized in quantitative yield from $Ru(DMF)_6^{3+}$ and are better defined starting materials with convenient intermediate substitution lability, no inert bonds such as Ru–Cl, and a well-defined oxidation state in comparison to the commonly used "Ru-blue" solution. The synthesis of new Ru–organic compounds through ligand exchange avoids sacrifice of the ligand normally required in order to reduce $RuCl_3 \cdot xH_2O$. Although $Ru(H_2O)_6^{2+}$ is useful for many classical syntheses, it has limited application under basic conditions because of hydrolysis of the ligand; thus the compounds **I** and **II** fill a gap in the range of starting materials available to the ruthenium chemist.

To our knowledge, there exist only two other crystal structure studies for hexakis(dimethylformamide) complexes, namely $[Si(DMF)_6]I_4$ and $[Fe^{III}(DMF)_6](ClO_4)_3$.[24,25] For these complexes and for **I** and **II**, an increase in the C–O distances (Si^{4+}, 1.26–1.28 Å; Fe^{3+}, 1.26–1.40 Å; Ru^{2+}, 1.22–1.24 Å; Ru^{3+}, 1.25–1.27 Å) and a decrease in the C–N distances (Si^{4+}, 1.26–1.49 Å; Fe^{3+}, 1.30–1.47 Å; Ru^{2+}, 1.30–1.42 Å; Ru^{3+}, 1.29–1.31 Å) as compared to those of free DMF (C–O = 1.17, C–N = 1.48 Å)[26] are observed. For **II**, the average ruthenium–oxygen distance of 2.088(9) Å compares with those of 2.122(16) Å in $Ru(H_2O)_6^{2+}$ [27] and 2.127 Å in $Ru(DMSO)_6^{2+}$ (DMSO = dimethyl sulfoxide).[28] The distances of Ru–O(water) and the Ru–O(DMSO) are slightly longer than that of Ru–O (DMF), which indicates a greater strength of binding of the DMF to Ru^{2+} in comparison with water and DMSO. For **I**, the average Ru–O distance of 2.02(2) Å can be compared with those in other $Ru^{III}O_6$ complexes, $Ru(H_2O)_6^{3+}$ (2.029(7) Å)[27] and $Ru(C_2O_4)_3^{3-}$ (2.028(4) Å).[29] In the delocalized acetylacetone complex $Ru(acac)_3$, the average Ru–O distance is 2.00(2) Å.[15]

Preliminary values for the rates of ligand exchange as measured by ^{1}H-NMR are, for **I**, $k_{ex}^{298} = 1.33 \times 10^{-6}$ s^{-1} and, for **II**, $k_{ex}^{298} = 1.53 \times 10^{-4}$ s^{-1}. The difference in the average metal–ligand bond distances between the $Ru(DMF)_6^{2+/3+}$ pair (0.07 Å) is slightly lower than the same value (0.09 Å) for the $Ru(H_2O)_6^{2+/3+}$ couple. The rate of electron transfer (self-exchange) for the $Ru(DMF)_6^{3+/2+}$ couple is therefore expected to be faster than the rate for the $Ru(H_2O)_6^{3+/2+}$ couple (20 s^{-1} M^{-1}).[30] Work is in progress to determine the activation parameters, including $\Delta V^{\ddagger}$, for solvent exchange and the electron self-exchange rate.[31]

Acknowledgment. We thank Dr. Christian Müller for his technical assistance with NMR spectroscopy and the Swiss National Science Foundation for supporting this research under Grant No. 203926893. We also thank CIBA for performing the microanalyses and Johnson-Matthey for a loan of ruthenium chloride.

Supporting Information Available: A full listing of anisotropic displacement parameters for the non-hydrogen atoms of **I** and **II** (Table S1 and S2), positional and isotropic displacement parameters for the hydrogen atoms of **I** (Table S3), and packing diagrams for **I** and **II** (Figures S1 and S2) (8 pages). Ordering information is given on any current masthead page.

IC950249V

(24) Deppisch, B.; Gladrow, B.; Kummer, D. *Z. Anorg. Allg. Chem.* **1984**, *519*, 42.
(25) Holt, E. M.; Alcock, N. W.; Sumner, R. H.; Asplund, R. O. *Cryst. Struct. Commun.* **1979**, *8*, 255.
(26) Vilkov, L. V.; Akishin, R. A.; Presynkova, V. M. *J. Struct. Chem.* **1962**, *3*, 3.
(27) Bernhard, P.; Bürgi, H.-B.; Hauser, J.; Lehmann, H.; Ludi, A. *Inorg. Chem.* **1982**, *21*, 3936.
(28) Davies, A. R.; Einstein, F. W. B.; Farrell, N. P.; James, B. R.; McMillan, R. S. *Inorg. Chem.* **1978**, *17*, 1965.
(29) Faure, R.; Duc, G.; Deloume, J.-P. *Acta Crystallogr.* **1986**, *C42*, 982.
(30) Bernhard, P.; Helm, L.; Ludi, A.; Merbach, A. *J. Am. Chem. Soc.* **1985**, *107*, 312.
(31) Cao, R.; Judd, R. J.; Ludi, A. *Book of Abstracts of the 5th International Conference on the Chemistry of the Platinum Group Metals*; Royal Society of Chemistry: St. Andrews, U.K., **1993**; p B.32.